Effects of interfacial friction on flaw tolerant adhesion between two dissimilar elastic solids

Citation: Yao, Haimin, and Huajian Gao. "Effects of Interfacial Friction on Flaw Tolerant Adhesion Between Two Dissimilar Elastic Solids." International Journal of Solids and Structures 46, no. 3–4 (February 2009): 860–870. © 2008 Elsevier Ltd.

As Published: http://dx.doi.org/10.1016/j.ijsolstr.2008.09.035

Publisher: Elsevier

Persistent URL: http://hdl.handle.net/1721.1/96331

Version: Final published version: final published article, as it appeared in a journal, conference proceedings, or other formally published context

International Journal of Solids and Structures 46 (2009) 860–870

Contents lists available at ScienceDirect

International Journal of Solids and Structures

journal homepage: www.elsevier.com/locate/ijsolstr

Effects of interfacial friction on flaw tolerant adhesion between two dissimilar elastic solids

Haimin Yao [a], Huajian Gao [b,*]

[a] Department of Materials Science and Engineering, Massachusetts Institute of Technology, 77 Massachusetts Avenue, MA 02139, USA
[b] Division of Engineering, Brown University, Providence, RI 02912, USA

ARTICLE INFO

Article history:
Received 29 July 2008
Received in revised form 18 September 2008
Available online 10 October 2008

Keywords:
Contact mechanics
Friction
Bimaterial interface
Hankel transform

ABSTRACT

Flaw tolerance refers to a state in which a pre-existing crack-like flaw does not propagate even as the material is stretched to failure near its theoretical strength. Such an optimal scenario can be achieved when the characteristic length scale is reduced to below a critical value. So far, the critical conditions to achieve flaw tolerance have been discussed mostly for homogeneous materials or for two dissimilar materials in frictionless or perfectly bonded adhesion. In this paper, we consider the role of friction in flaw tolerant adhesion between two dissimilar elastic solids. We adopt a frictional contact model in which slip is allowed wherever the shear stress along the interface reaches a threshold value defined as the friction strength. The critical length scale for flaw tolerance is derived analytically for a penny-shaped crack and for an external circular crack. Compared to the cases of frictionless contact, we find that interfacial friction can reduce the critical length scales for flaw tolerance by up to 12.5%.

1. Introduction

The *theoretical strength* of brittle solids, defined as the stress required to simultaneously break all atomic bonds across a failure plane, is around one tenth of Young's modulus. In reality, however, such a high strength is rarely observed due to the presence of crack-like flaws. Upon external loading, stress concentration tends to occur near crack tips. As the applied load is increased to a value usually much lower than the theoretical strength, a critical crack-like flaw begins to propagate and the solid fails by crack propagation instead of simultaneous failure of all bonds along the prospective failure plane. Similar process can be observed in adhesion. For two solids sticking to one another via, for example, the van der Waals interaction, crack-like flaws induced by surface roughness, impurities and contaminants induce severe stress concentration near the edges of contact zones. As the applied load is increased to a critical value, the adhesion joint fails by crack propagation rather than simultaneous failure of interface at the theoretical strength of van der Waals interaction. In these failure processes dominated by crack propagation, the load carrying capacity of material has not been fully utilized since only a small fraction of material is highly stressed at any instant of time.

The state of *flaw tolerance* is defined as such that a pre-existing crack does not propagate even as the material is stretched to failure near the theoretical strength. In this case, material around the crack fails not by crack propagation but rather by uniform rupture at the theoretical strength. How can we achieve such an optimal scenario? This question has aroused considerable interest in recent studies on the mechanical properties of biological materials. For example, Gao et al. (2003, 2004) investigated the nanoscale mechanical properties of bone and bone-like materials, and showed that the nanometer size of "mineral" crystals plays a critical role in the strength and toughness of bone. Gao and Chen (2005) considered the tensile strength of a cracked elastic strip and showed that the strip becomes flaw tolerant as long as its half-width h meets the condition

* Corresponding author. Tel.: +1 401 863 2626; fax: +1 401 863 9052.
E-mail address: Huajian_Gao@brown.edu (H. Gao).

0020-7683/$ - see front matter © 2008 Elsevier Ltd. All rights reserved.
doi:10.1016/j.ijsolstr.2008.09.035

$$h \leqslant h_{cr} = \frac{\Gamma E}{S^2}, \tag{1}$$

where E is Young's modulus, S and Γ stand for the theoretical strength and fracture energy of the strip, respectively. For brittle materials, Γ is commonly taken as twice of the surface energy, i.e. $\Gamma = 2\gamma$.

Studies on biological attachment systems (Autumn et al., 2000; Arzt et al., 2003; Gao and Yao, 2004) have also inspired interests in flaw tolerant adhesion. Gao et al. (2005) performed finite element calculations to show that the adhesion strength of a flat-ended cylindrical punch in partial contact with a rigid substrate would saturate at its theoretical strength when the size of the punch is reduced to below a critical radius. Such saturation of adhesion strength at small length scale has also been reported by Persson (2003) for a rigid cylindrical punch on an elastic half-space and by Tang (2005) for an elastic cylindrical punch in perfect bonding with a rigid substrate. All these models agree on the point that there exists a critical length scale for flaw tolerant adhesion which is proportional to $\Delta\gamma E^*/\sigma_{th}^2$, where $\Delta\gamma$ is the work of adhesion, $E^* = [(1-\nu_1^2)/E_1 + (1-\nu_2^2)/E_2]^{-1}$ is the compound modulus and σ_{th} is the theoretical adhesion strength. In reality, however, adhesive contact is neither frictionless nor perfectly bonded. Interfacial slip is expected to occur along the interface wherever shear stresses are too high. To understand the role of friction in flaw tolerant adhesion, in this paper we consider adhesive contact between two dissimilar elastic solids in which slip is allowed along the contact interface wherever the shear stress reaches a threshold value defined as the friction strength of the interface. The critical length scale for flaw tolerant adhesion will be determined analytically for a penny-shaped crack and an external circular crack along a frictional interface between two dissimilar elastic solids.

2. Frictional contact model

Penny-shaped cracks and external circular cracks are two typical crack configurations that can arise along a contact interface between two elastic solids. While the former represents a circular unbonded region along an otherwise bonded interface (Fig. 1a), the latter (Fig. 2a) refers to a circular ligament that connects two otherwise separate solids. For simplicity, we treat the contacting solids as two elastic half-spaces and adopt Dugdale's interaction law (1960)

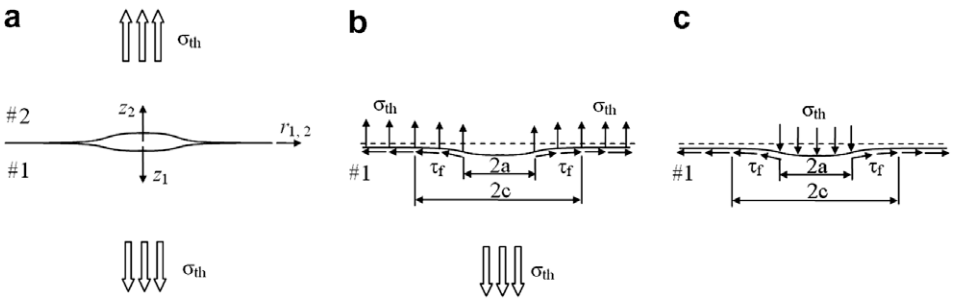

Fig. 1. Flaw tolerant solution for a penny-shaped crack along a frictional contact interface between two dissimilar elastic solids. (a) The crack configuration and the coordinate systems adopted in the study. (b) Surface tractions on material #1 in the flaw tolerance state. The normal traction at pull-off is uniform and equal to the theoretical strength σ_{th} over the entire contact region outside the crack. The friction stress is equal to τ_f in the slip region ($a \leqslant r \leqslant c$) and remains to be determined in the non-slip region ($c < r < \infty$). (c) Superposition of a uniform pressure σ_{th} converts the original problem into a simpler one.

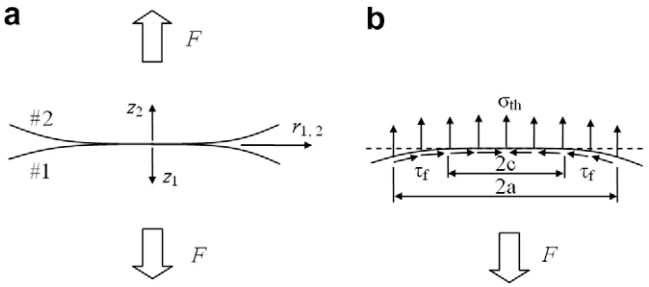

Fig. 2. Flaw tolerant solution to frictional contact between two dissimilar elastic solids over a circular ligament. (a) The crack configuration and the coordinate systems adopted in the study. (b) Surface tractions on material #1 in the flaw tolerance state. The normal traction at pull-off is uniform and equal to the theoretical strength σ_{th} over the entire circular ligament. The friction stress is equal to τ_f in the slip region ($c \leqslant r \leqslant a$) and remains to be determined in the non-slip region ($0 \leqslant r \leqslant c$).

$$\sigma = \begin{cases} \sigma_{th} & (\delta \leqslant \Delta\gamma/\sigma_{th}), \\ 0 & (\delta > \Delta\gamma/\sigma_{th}), \end{cases} \tag{1}$$

for the normal traction σ along the interface, where δ is the surface separation between the two solids. Use of more realistic interaction laws generally yields results qualitatively similar to those derived based on the Dugdale model (Barthel, 1998). We consider a frictional contact model in which slip is allowed along the interface wherever the shear stress reaches the friction strength τ_f. Therefore, the contact area is divided into a *slip region*, in which the shear stress is equal to the friction strength τ_f and a *non-slip region*, in which the shear stress is smaller than τ_f. We are interested in the flaw tolerance solution in which the normal traction outside the crack region is uniform and equal to the theoretical strength σ_{th}, as depicted in Figs. 1b and 2b for a penny-shaped crack and an external circular crack, respectively. According to Dugdale's interaction law, the flaw tolerant solution exist as long as

$$\delta_{tip} \leqslant \frac{\Delta\gamma}{\sigma_{th}}, \tag{2}$$

where δ_{tip} stands for the crack tip opening displacement. Since δ_{tip} is usually a monotonically increasing function of the crack size a, Eq. (2) suggests that there might be a critical crack size a_{cr} below which flaw-tolerant adhesion becomes possible. In the following, we show that this is indeed the case and will determine the critical length scales of flaw tolerance for a penny-shaped crack and for an external circular crack along a frictional contact interface.

3. Flaw tolerant solution to a penny-shaped crack along a frictional contact interface

Consider the flaw tolerance state of a penny-shaped crack along a frictional contact interface. Fig. 1b shows the tractions acting on the surface of material #1 at pull-off. While the normal traction is uniform and equal to the theoretical strength of adhesion σ_{th} over the entire contact region ($a \leqslant r \leqslant \infty$), the shear traction is equal to the friction strength τ_f in the slip region ($a < r < c$) but remains to be determined in the non-slip region ($c < r < \infty$). Before proceeding to calculate the shear stress in the non-slip region, we superpose a uniform pressure σ_{th} on the whole surface (Fig. 1b). This treatment does not affect the condition for flaw tolerance but converts the original problem into a simpler one shown in Fig. 1c.

According to the general solutions to axisymmetric problems of an elastic half-space (see Appendix A), the displacement and stress components on the surfaces ($z = 0$) of material #1 and #2 can be expressed in terms of their Hankel transforms as

$$u_r^{(1)}(r,0) = \frac{1}{2\mu_1}\mathcal{H}_1[\xi^{-1}C_1;\xi\to r], \tag{3a}$$

$$\tau_{zr}^{(1)}(r,0) = -\mathcal{H}_1[(1-2\nu_1)A_1 + C_1;\xi\to r], \tag{3b}$$

$$\sigma_{zz}^{(1)}(r,0) = -\mathcal{H}_0[(2-2\nu_1)A_1 + C_1;\xi\to r], \tag{3c}$$

and

$$u_r^{(2)}(r,0) = \frac{1}{2\mu_2}\mathcal{H}_1[\xi^{-1}C_2;\xi\to r], \tag{4a}$$

$$\tau_{zr}^{(2)}(r,0) = -\mathcal{H}_1[(1-2\nu_2)A_2 + C_2;\xi\to r], \tag{4b}$$

$$\sigma_{zz}^{(2)}(r,0) = -\mathcal{H}_0[(2-2\nu_2)A_2 + C_2;\xi\to r], \tag{4c}$$

where μ_1,μ_2 are shear moduli, ν_1,ν_2 are Poisson's ratios and A_1,A_2,C_1,C_2 are functions of ξ to be determined from boundary conditions. It should be pointed out that the displacement and stress components in Eqs. (3) and (4) are referred to separate coordinate systems for each material as shown in Fig. 1a. Since the tractions on the two contacting surfaces are equal and opposite, we have

$$\sigma_{zz}^{(1)}(r,0) = \sigma_{zz}^{(2)}(r,0), \quad \tau_{zr}^{(1)}(r,0) = -\tau_{zr}^{(2)}(r,0). \tag{5}$$

Inserting Eqs. (3) and (4) into Eq. (5) gives rise to

$$(2-2\nu_1)A_1 + C_1 = (2-2\nu_2)A_2 + C_2, \tag{6}$$

$$(1-2\nu_1)A_1 + C_1 = -(1-2\nu_2)A_2 - C_2, \tag{7}$$

which suggest that C_2 can be expressed in terms of A_1 and C_1 as

$$-C_2 = \frac{A_1}{2}[\kappa_1\kappa_2 - 1] + \kappa_2 C_1, \tag{8}$$

where $\kappa_i = 3 - 4\nu$ ($i = 1,2$).

In the non-slip region, the relative displacement between the two surfaces should vanish, i.e.

$$u_r^{(1)}(r,0) - u_r^{(2)}(r,0) = 0 \quad (r > c). \tag{9}$$

Substituting Eqs. (3a) and (4a) into Eq. (9) yields

$$\mathcal{H}_1\left[\xi^{-1}\left(\frac{C_1}{\mu_1}-\frac{C_2}{\mu_2}\right);\xi\to r\right]=0\quad(r>c). \tag{10}$$

Recalling Eq. (8), Eq. (10) can be rewritten as

$$\mathcal{H}_1[\xi^{-1}(C_1+\alpha A_1);\xi\to r]=0\quad(r>c), \tag{11}$$

where $\alpha=\dfrac{(\kappa_1\kappa_2-1)\mu_1}{2(\mu_2+\mu_1\kappa_2)}$.

For material #1, the stress boundary conditions are given by

$$\sigma_{zz}^{(1)}(r,0)=T(r/c)\quad(0\leqslant r<\infty), \tag{12}$$

$$\tau_{rz}^{(1)}(r,0)=Q(r/c)\quad(0\leqslant r\leqslant c), \tag{13}$$

where

$$T(r/c)=\begin{cases}0 & (a<r<\infty),\\ -\sigma_{th} & (0\leqslant r\leqslant a),\end{cases} \tag{14}$$

and

$$Q(r/c)=\begin{cases}-\tau_f & (a\leqslant r\leqslant c),\\ 0 & (0\leqslant r\leqslant a).\end{cases} \tag{15}$$

Inserting Eqs. (3b) and (3c) into (12) and (13) yields

$$\sigma_{zz}^{(1)}(r,0)=-\mathcal{H}_0[(2-2\nu_1)A_1+C_1;\xi\to r]=T(\rho)\quad(0\leqslant r<\infty), \tag{16}$$

$$\tau_{zr}^{(1)}(r,0)=-\mathcal{H}_1[(1-2\nu_1)A_1+C_1;\xi\to r]=Q(\rho)\quad(0\leqslant r\leqslant c), \tag{17}$$

where $\rho = r/c$.

Introducing two auxiliary functions $\phi(\xi) = C_1(\xi/c)$, $\psi(\xi) = A_1(\xi/c)$, Eqs. (11), (16) and (17) can be normalized as

$$\mathcal{H}_1[\xi^{-1}[\phi(\xi)+\alpha\psi(\xi)];\xi\to\rho]=0\quad(1<\rho<\infty), \tag{18}$$

$$\mathcal{H}_0[(2-2\nu_1)\psi(\xi)+\phi(\xi);\xi\to\rho]=-c^2T(\rho)\quad(0\leqslant\rho<\infty), \tag{19}$$

$$\mathcal{H}_1[(1-2\nu_1)\psi(\xi)+\phi(\xi);\xi\to\rho]=-c^2Q(\rho)\quad(0\leqslant\rho\leqslant 1). \tag{20}$$

As Eq. (19) holds for the whole surface, substituting Eq. (14) into Eq. (19) and then performing inverse Hankel transform on both sides gives the following relationship between $\psi(\xi)$ and $\phi(\xi)$ as

$$(2-2\nu_1)\psi(\xi)+\phi(\xi)=ca\sigma_{th}\xi^{-1}J_1(a\xi/c)\quad(0\leqslant\rho<\infty). \tag{21}$$

Substituting Eq. (21) back into Eqs. (18) and (20) to eliminate function $\phi(\xi)$ results in two equations with respective to $\psi(\xi)$ as

$$\mathcal{H}_1[\xi^{-1}\psi(\xi);\xi\to\rho]=-\frac{a^2\sigma_{th}}{2[\alpha-(2-2\nu_1)]\rho}\quad(\rho>1), \tag{22}$$

$$\mathcal{H}_1[\psi(\xi);\xi\to\rho]=c^2Q(\rho)+ac\sigma_{th}H_1\left[\frac{J_1(a\xi/c)}{\xi};\xi\to\rho\right]\quad(0\leqslant\rho\leqslant 1). \tag{23}$$

Eq. (23) implies that the function $\psi(\xi)$ should have the form

$$\psi(\xi)=ac\sigma_{th}\frac{J_1(a\xi/c)}{\xi}+\bar{\psi}(\xi), \tag{24}$$

where function $\bar{\psi}(\xi)$, according to Eqs. (22) and (23), is determined by

$$\mathcal{H}_1[\bar{\psi}(\xi);\xi\to\rho]=c^2Q(\rho)\quad(0\leqslant\rho\leqslant 1), \tag{25}$$

$$\mathcal{H}_1[\xi^{-1}\bar{\psi}(\xi);\xi\to\rho]=-\frac{a^2\sigma_{th}\beta}{\rho}\quad(\rho>1). \tag{26}$$

Here

$$\beta=\frac{1}{2}\frac{(\kappa_1-1)/\mu_1-(\kappa_2-1)/\mu_2}{(\kappa_1+1)/\mu_1+(\kappa_2+1)/\mu_2} \tag{27}$$

is one of Dundurs' constants (1969) for the bimaterial, which has an admissible range of $-0.25\leqslant\beta\leqslant 0.25$. The more dissimilar the materials, the larger the absolute value of β.

Eqs. (25) and (26) are typical dual integral equations, whose solution can be obtained directly from Sneddon's general solution (1966) as (see Appendix B)

$$\bar{\psi}(\xi) = -\tau_f c^2 \frac{2}{\pi} \int_{a/c}^{1} \frac{1}{t} \left(\frac{\sin \xi t}{\xi t} - \cos \xi t \right) dt \int_{a/c}^{t} \frac{\tau^2}{\sqrt{t^2 - \tau^2}} d\tau - \frac{a^2 \sigma_{th} \beta \sin \xi}{\xi}. \tag{28}$$

According to Eqs. (3b), (21) and (24), the friction stress can be expressed in terms of $\bar{\psi}(\xi)$ as

$$\tau_{zr}^{(1)}(r,0) = \frac{1}{c^2} \mathcal{H}_1[\bar{\psi}(\xi); \xi \to \rho], \tag{29}$$

which upon the substitution of Eq. (28) yields

$$\tau_{zr}^{(1)}(r,0) = \frac{1}{c^2} \left[\frac{2c^2 \tau_f}{\pi \rho \sqrt{\rho^2 - 1}} \int_{a/c}^{1} \frac{t^2 \sqrt{1 - t^2}}{\rho^2 - t^2} dt - \frac{a^2 \sigma_{th} \beta}{\rho \sqrt{\rho^2 - 1}} \right] \quad (\rho > 1). \tag{30}$$

The continuity of friction stress in the contact region requires that the singularity in Eq. (30) at $\rho = 1$ vanish, which gives the following implicit relationship between the ratio of a/c and $\pi \sigma_{th} \beta / \tau_f$:

$$\sqrt{\frac{c^2}{a^2} - 1} + \frac{c^2}{a^2} \cos^{-1} \left(\frac{a}{c} \right) = \frac{\pi \sigma_{th} \beta}{\tau_f}. \tag{31}$$

In addition, Eq. (31) also demands that $\beta/\tau_f \geqslant 0$, which means that the sign (or direction) of the frictional stress is correlated with the sign of β. The stress directions depicted in Fig. 1a corresponds to $\beta \geqslant 0$. In our analysis we assume $\beta \geqslant 0$ and $\tau_f > 0$, which does not lead to any loss of generality considering the exchangeability of material #1 and #2.

Substituting Eq. (31) into Eq. (30) gives the friction stress in the non-slip region as

$$\tau_{zr}^{(1)}(r,0) = \frac{2\tau_f \sqrt{\rho^2 - 1}}{\pi \rho} \cos^{-1} \left(\frac{a}{c} \right) - \frac{\tau_f}{\pi} \left[\cos^{-1} \left(\frac{\rho a - c}{\rho c - a} \right) + \cos^{-1} \left(\frac{\rho a + c}{\rho c + a} \right) \right] \quad (\rho > 1). \tag{32}$$

We have thus obtained all of the tractions acting on material #1:

$$\begin{cases} \sigma_{zz}(r,0) = -\sigma_{th} & (0 \leqslant r \leqslant a), \\ \tau_{zr}(r,0) = \dfrac{2\tau_f \sqrt{\rho^2 - 1}}{\pi \rho} \cos^{-1} \left(\dfrac{a}{c} \right) - \dfrac{\tau_f}{\pi} \left[\cos^{-1} \left(\dfrac{\rho a - c}{\rho c - a} \right) + \cos^{-1} \left(\dfrac{\rho a + c}{\rho c + a} \right) \right] & (c < r < \infty), \\ \tau_{zr}(r,0) = -\tau_f & (a \leqslant r \leqslant c). \end{cases} \tag{33}$$

The normal surface displacement of material #1 at crack tip $r = a$ is (Johnson, 1985)

$$\delta_{tip}^{(1)} = \frac{4\sigma_{th} a (1 - \nu_1^2)}{\pi E_1} + \frac{(1 - 2\nu_1)(1 + \nu_1) \tau_f c}{\pi E_1} \cos^{-1} \left(\frac{a}{c} \right). \tag{34}$$

Considering the fact that the tractions applied on material #2 are equal and opposite to those on material #1, according to Eq. (34), the surface displacement of material #2 at $r = a$ is

$$\delta_{tip}^{(2)} = \frac{4\sigma_{th} a (1 - \nu_2^2)}{\pi E_2} - \frac{(1 - 2\nu_2)(1 + \nu_2) \tau_f c}{\pi E_2} \cos^{-1} \left(\frac{a}{c} \right). \tag{35}$$

The total crack tip opening displacement is thus

$$\delta_{tip} = \delta_{tip}^{(1)} + \delta_{tip}^{(2)} = \frac{4\sigma_{th} a}{\pi E^*} + \frac{4\beta \tau_f c}{\pi E^*} \cos^{-1} \left(\frac{a}{c} \right), \tag{36}$$

where $E^* = [(1 - \nu_1^2)/E_1 + (1 - \nu_2^2)/E_2]^{-1}$. Substituting Eq. (36) into Eq. (2) yields the critical radius of the penny-shaped crack to achieve flaw tolerance as

$$a_{cr}^{fn} = \frac{1}{1 + \dfrac{c\beta\tau_f}{a\sigma_{th}} \cos^{-1} \left(\dfrac{a}{c} \right)} a_{cr}^{fl}, \tag{37}$$

where $a_{cr}^{fl} = \pi E^* \Delta\gamma / 4\sigma_{th}^2$ is the critical radius in the frictionless case $\beta\tau_f = 0$. Note that the ratio a/c has been determined from Eq. (31). Variation of a/c as a function of β for different values of shear-to-normal strength ratio τ_f/σ_{th} is shown in Fig. 3a.

4. Flaw tolerant solution to frictional contact between two dissimilar elastic solids over a circular ligament

Similar solution process applies to the problem of frictional contact between two dissimilar elastic solids over a circular ligament, corresponding to an external circular crack. In this case, the boundary conditions can be expressed in terms of Hankel transforms as

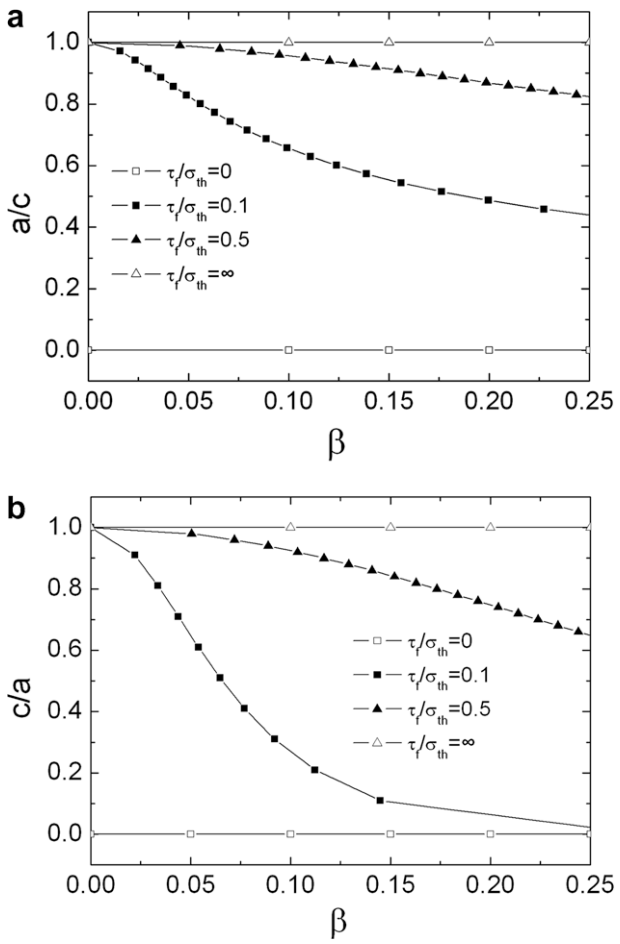

Fig. 3. Variation of a/c (or c/a) as a function of Dundurs' constant β for different values of shear-to-normal strength ratio τ_f/σ_{th}: (a) the penny-shaped crack and (b) external circular crack.

$$\mathcal{H}_1[\xi^{-1}(C_1+\alpha A_1);\xi\to r]=0 \quad (0\leqslant r\leqslant c), \tag{38}$$

$$\sigma_{zz}^{(1)}(r,0)=-\mathcal{H}_0[(2-2\nu_1)A_1+C_1;\xi\to r]=T(\rho) \quad (0\leqslant r<\infty), \tag{39}$$

$$\tau_{zr}^{(1)}(r,0)=-\mathcal{H}_1[(1-2\nu_1)A_1+C_1;\xi\to r]=Q(\rho) \quad (c<r<\infty), \tag{40}$$

where

$$T(r/c)=\begin{cases}0 & (a<r<\infty),\\ \sigma_{th} & (0\leqslant r\leqslant a),\end{cases} \tag{41}$$

and

$$Q(r/c)=\begin{cases}\tau_f & (c\leqslant r\leqslant a),\\ 0 & (a<r<\infty).\end{cases} \tag{42}$$

Likewise, by introducing the auxiliary functions $\phi(\xi)=C_1(\xi/c)$ and $\psi(\xi)=A_1(\xi/c)$, Eqs. (38)–(40) can be normalized as

$$\mathcal{H}_1[\xi^{-1}[\phi(\xi)+\alpha\psi(\xi)];\xi\to\rho]=0 \quad (0\leqslant\rho\leqslant 1), \tag{43}$$

$$\mathcal{H}_0[(2-2\nu_1)\psi(\xi)+\phi(\xi);\xi\to\rho]=-c^2T(\rho) \quad (0\leqslant\rho<\infty), \tag{44}$$

$$\mathcal{H}_1[(1-2\nu_1)\psi(\xi)+\phi(\xi);\xi\to r]=-c^2Q(\rho) \quad (1<\rho<\infty). \tag{45}$$

Since Eq. (44) is defined over the whole surface, substituting Eq. (41) into (44) and then performing inverse Hankel transform on both sides lead to the following relationship between functions $\psi(\xi)$ and $\phi(\xi)$:

$$(2-2\nu_1)\psi(\xi)+\phi(\xi)=-c^2\sigma_{th}\int_0^{a/c}\rho J_0(\rho\xi)d\rho=-ca\sigma_{th}\xi^{-1}J_1(a\xi/c). \tag{46}$$

Inserting Eq. (46) back into Eqs. (43) and (45) to eliminate the function $\phi(\xi)$, we have

$$\mathcal{H}_1[\xi^{-1}\psi(\xi);\xi\to\rho]=\frac{c^2\sigma_{th}\rho}{2[\alpha-(2-2\nu_1)]}\quad(0\leqslant\rho\leqslant 1), \tag{47}$$

$$\mathcal{H}_1[\psi(\xi);\xi\to\rho]=c^2Q(\rho)-ca\sigma_{th}\mathcal{H}_1[\xi^{-1}J_1(a\xi/c);\xi\to\rho]\quad(1<\rho<\infty). \tag{48}$$

Eq. (48) implies that $\psi(\xi)$ should have the form

$$\psi(\xi)=-ca\sigma_{th}\xi^{-1}J_1(a\xi/c)+\bar{\psi}(\xi), \tag{49}$$

where $\bar{\psi}(\xi)$, according to Eqs. (47) and (48), satisfies

$$\mathcal{H}_1[\xi^{-1}\bar{\psi}(\xi);\xi\to\rho]=c^2\sigma_{th}\beta\rho\quad(0\leqslant\rho\leqslant 1), \tag{50}$$

$$\mathcal{H}_1[\bar{\psi}(\xi);\xi\to\rho]=c^2Q(\rho)\quad(1<\rho<\infty). \tag{51}$$

For dual integral equations (50) and (51), the solution can also be derived directly from Sneddon's general solution (1966). The result is given by (see Appendix C)

$$\bar{\psi}(\xi)=\frac{2}{\pi}c^2\tau_f\int_1^{a/c}t\ln\left[\frac{a}{tc}+\sqrt{\frac{a^2}{c^2t^2}-1}\right]\sin(\xi t)dt+\frac{4}{\pi}c^2\sigma_{th}\beta\left(\frac{\sin\xi}{\xi^2}-\frac{\cos\xi}{\xi}\right). \tag{52}$$

The friction stress can be obtained as

$$\tau_{zr}^{(1)}(r,0)=\frac{1}{c^2}\mathcal{H}_1[\bar{\psi}(\xi);\xi\to\rho]=\frac{2}{\pi}\left[-\frac{\tau_f\rho}{\sqrt{1-\rho^2}}\int_1^{a/c}\frac{(t^2-1)^{1/2}dt}{t^2-\rho^2}+2\sigma_{th}\beta\frac{\rho}{\sqrt{1-\rho^2}}\right]. \tag{53}$$

The continuity of friction stress in the ligament implies no singularity in Eq. (53) as $\rho\to 1$, giving the following implicitly relationship

$$\frac{a}{c}+\sqrt{\frac{a^2}{c^2}-1}=\exp\left(\frac{2\sigma_{th}\beta}{\tau_f}\right) \tag{54}$$

between $2\sigma_{th}\beta/\tau_f$ and a/c. Since $a/c>1$ in Eq. (54), it follows that $\beta/\tau_f\geqslant 0$, indicating that the frictional stress should have the same sign as β. The direction of friction stress shown in Fig. 1b corresponds to $\beta\geqslant 0$, which is assumed without loss of generality.

Inserting Eq. (54) into (53) leads to

$$\tau_{rz}^{(1)}(r,0)=\frac{\tau_f}{\pi}\left[\sin^{-1}\left(\frac{ra-c^2}{ac-rc}\right)+\sin^{-1}\left(\frac{ra+c^2}{ac+rc}\right)\right]. \tag{55}$$

The tractions acting on material #1 are given by

$$\begin{cases}\sigma_{zz}^{(1)}(r,0)=\sigma_{th} & (0\leqslant r\leqslant a),\\ \tau_{zr}^{(1)}(r,0)=\dfrac{\tau_f}{\pi}\left[\sin^{-1}\left(\dfrac{ra-c^2}{ac-rc}\right)+\sin^{-1}\left(\dfrac{ra+c^2}{ar+rc}\right)\right] & (0\leqslant r<c),\\ \tau_{zr}^{(1)}(r,0)=\tau_f & (c\leqslant r\leqslant a).\end{cases} \tag{56}$$

The corresponding normal surface displacements on materials #1 and #2 are (Johnson, 1985)

$$u_z^{(1)}(r,0)=-\frac{4\sigma_{th}a}{\pi E_1^*}\mathbf{E}\left(\frac{r}{a}\right)-\frac{2(\kappa_1-1)\tau_f(a-c)}{\pi(\kappa_1+1)E_1^*}-\frac{2(\kappa_1-1)\tau_f c}{\pi^2(\kappa_1+1)E_1^*}\times\left[\pi-\frac{r}{c}\sin^{-1}\left(\frac{ra-c^2}{ac-rc}\right)-\frac{r}{c}\sin^{-1}\left(\frac{ra+c^2}{ac+rc}\right)-2\frac{a}{c}\sin^{-1}\left(\sqrt{\frac{c^2-r^2}{a^2-r^2}}\right)\right]\quad(0\leqslant r<c), \tag{57}$$

$$u_z^{(1)}(r,0)=-\frac{4\sigma_{th}a}{\pi E_1^*}\mathbf{E}\left(\frac{r}{a}\right)-\frac{2(\kappa_1-1)\tau_f(a-r)}{\pi(\kappa_1+1)E_1^*}\quad(c\leqslant r\leqslant a), \tag{58}$$

where $E_1^*=E_1/(1-\nu_1^2)$ and $\mathbf{E}(\cdot)$ is the complete elliptical integral of the second kind.

For the external circular crack, the crack tip opening displacement contributed by material #1 is equal to the relative normal displacement between contact edge ($r=a$) and center ($r=0$), i.e.

$$\delta_{tip}^{(1)}=|u_z^{(1)}(a,0)-u_z^{(1)}(0,0)|. \tag{59}$$

Inserting Eqs. (57) and (58) into Eq. (59) leads to

$$\delta_{tip}^{(1)}=\frac{2\sigma_{th}a}{E_1^*}\left(1-\frac{2}{\pi}\right)+\frac{2(\kappa_1-1)\tau_f a}{\pi(\kappa_1+1)E_1^*}\left[1-\frac{2}{\pi}\sin^{-1}\left(\frac{c}{a}\right)\right]. \tag{60}$$

Likewise, the crack opening contributed by material #2 is obtained as

$$\delta_{tip}^{(2)} = \frac{2\sigma_{th}a}{E_2^*}\left(1-\frac{2}{\pi}\right) - \frac{2(\kappa_2-1)\tau_f a}{\pi(\kappa_2+1)E_2^*}\left[1-\frac{2}{\pi}\sin^{-1}\left(\frac{c}{a}\right)\right]. \tag{61}$$

The total crack tip opening displacement is

$$\delta_{tip} = \delta_{tip}^{(1)} + \delta_{tip}^{(2)} = \frac{2\sigma_{th}a}{\pi E^*}(\pi-2) + \frac{8\tau_f a\beta}{\pi^2 E^*}\cos^{-1}\left(\frac{c}{a}\right). \tag{62}$$

Substituting Eq. (62) into Eq. (2) gives rise to the critical size for the circular ligament to achieve flaw tolerance as

$$a_{cr}^{fn} = \frac{(\pi-2)}{(\pi-2)+\frac{4\beta\tau_f}{\pi\sigma_{th}}\cos^{-1}(c/a)}a_{cr}^{fl}, \tag{63}$$

where $a_{cr}^{fl} = \pi E^*\Delta\gamma/2\sigma_{th}^2(\pi-2)$ is the critical radius in the frictionless case $\beta\ \tau_f = 0$. Note that the ratio c/a has been determined by Eq. (54). Variation of c/a as a function of β for different values of shear-to-normal strength ratio τ_f/σ_{th} is shown in Fig. 3b.

5. Discussions and conclusions

For both internal and external circular crack configurations along a frictional contact interface, Eqs. (37) and (63) show that the critical length scales for flaw tolerance are proportional to $\Delta\gamma E^*/\sigma_{th}^2$, in agreement with previous results based on the frictionless assumption (Persson, 2003; Gao et al., 2005). The influence of friction on the critical length scales for flaw tolerance can be seen from the ratio a_{cr}^{fn}/a_{cr}^{fl} which is plotted in Fig. 4 as a function of the Dundurs' constant β for different

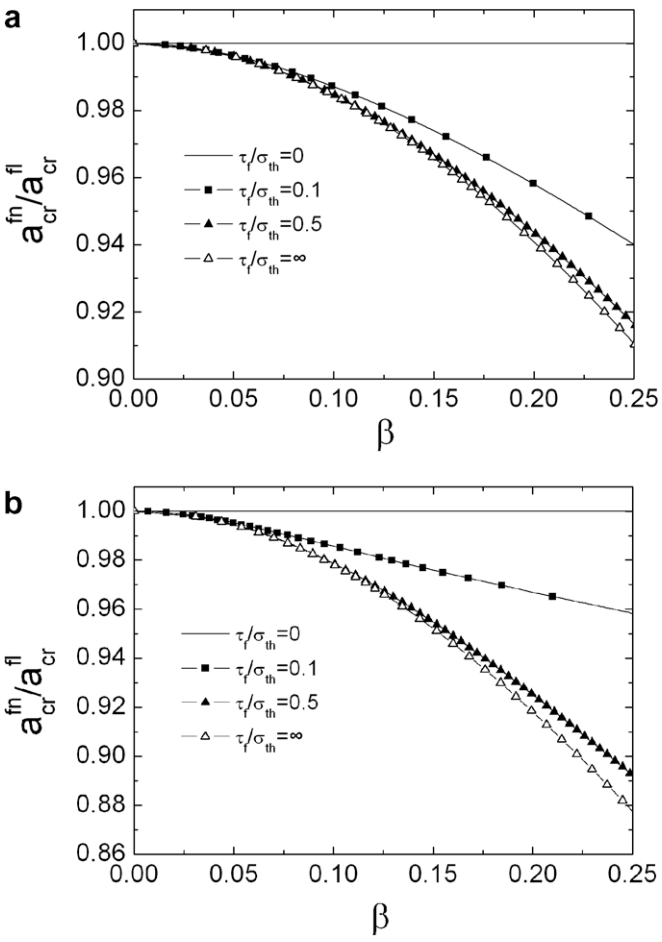

Fig. 4. The normalized critical length scale for flaw tolerance a_{cr}^{fn}/a_{cr}^{fl} as a function of the Dundurs' constant β for different values of the shear-to-normal strength ratio τ_f/σ_{th}: (a) penny-shaped crack and (b) external circular crack.

values of the shear-to-normal strength ratio τ_f/σ_{th}. Considering the symmetry of the results with respect to $\beta = 0$, here we just show the results in the range of $0 \leqslant \beta \leqslant 0.25$. For both internal and external circular cracks, it can be seen that the existence of interfacial friction can reduce the critical length scale for flaw tolerance by up to 12.5%. For fixed β, higher τ_f/σ_{th} leads to smaller critical length scale, implying that friction is unfavorable for flaw tolerance. On the other hand, for τ_f/σ_{th}, the critical length scale for flaw tolerance decreases as β increases, suggesting that elastic dissimilarity is also unfavorable for flaw tolerance. These results suggest that the concept of flaw tolerant adhesion at sufficiently small length scales is valid also for frictional contact two dissimilar elastic solids. Furthermore, friction and elastic dissimilarity can have moderate effects (up to 12.5%) on the critical length scales for flaw tolerance.

Appendix A. Solutions to axisymmetric problems of an elastic half-space via Hankel transform

The Papkovich–Neuber solution (Gladwell, 1980) in the classical theory of elasticity gives the following general displacement solutions to axisymmetric problems in cylindrical coordinate system with z-direction pointing into the solid interior,

$$u_r = -\frac{1}{2\mu}\frac{\partial}{\partial r}(z\Psi + \Phi), \tag{A1}$$

$$u_z = \frac{1}{2\mu}\left[4(1-\nu)\Psi - \frac{\partial}{\partial z}(z\Psi + \Phi)\right], \tag{A2}$$

$$u_\theta = 0, \tag{A3}$$

where μ is the shear modulus and Ψ, Φ are two harmonic functions satisfying

$$\nabla^2\Psi = 0, \tag{A4}$$

$$\nabla^2\Phi = 0. \tag{A5}$$

The exact forms of Ψ, Φ are to be determined by the specific boundary conditions.

On the other hand, for an arbitrary harmonic function $\Psi(r,z)$, the following equation is satisfied:

$$\mathcal{H}_0[\nabla^2\Psi(r,z); r \to \xi] = (D_z^2 - \xi^2)\overline{\Psi}(\xi,z) = 0, \tag{A6}$$

where

$$\overline{\Psi}(\xi,z) = \mathcal{H}_0[\Psi(r,z); r \to \xi], \tag{A7}$$

$$D_z = \frac{\partial}{\partial z}. \tag{A8}$$

Here, $\mathcal{H}_n$ is the *Hankel transform* of order n defined by

$$\mathcal{H}_n[f(r); r \to \xi] = \int_0^\infty rf(r)J_n(r\xi)dr \tag{A9}$$

with inverse given by

$$\mathcal{H}_n^{-1}[H(\xi); \xi \to r] = \int_0^\infty \xi H(\xi)J_n(\xi r)d\xi, \tag{A10}$$

where $J_n(r)$ is the Bessel function of the first kind with order n. Given that Ψ is finite as $z \to \infty$, the solution to Eq. (A6) is given by

$$\overline{\Psi}(\xi,z) = \xi^{-1}A(\xi)\exp(-\xi z), \tag{A11}$$

where $A(\xi)$ is an arbitrary function with respect to ξ.

Performing inverse Hankel transform on Eq. (A11) leads to the expression of an arbitrary harmonic function $\Psi(r,z)$ in terms of Hankel transform as

$$\Psi(r,z) = \mathcal{H}_0[\xi^{-1}A(\xi)\exp(-\xi z); \xi \to r]. \tag{A12}$$

Similarly, we can also express harmonic function $\Phi(r,z)$ in terms of Hankel transform as

$$\Phi(r,z) = \mathcal{H}_0[\xi^{-2}C(\xi)\exp(-\xi z); \xi \to r], \tag{A13}$$

where $C(\xi)$ are arbitrary functions with respect to ξ.

By substituting Eqs. (A12) and (A13) into Eqs. (A1)–(A3) and then applying the following relationship between Hankel transforms H_0 and H_1 for arbitrary function $g(\xi)$,

$$\frac{\partial}{\partial r}\mathcal{H}_0[g(\xi); \xi \to r] = -\mathcal{H}_1[\xi g(\xi); \xi \to r], \tag{A14}$$

the displacement and stress fields for an axisymmetric problem of elastic half-space can be expressed as

$$u_r(r,z) = \mathcal{H}_1[U(\xi,z);\xi\to r], \tag{A15}$$
$$u_z(r,z) = \mathcal{H}_0[V(\xi,z);\xi\to r], \tag{A16}$$
$$\tau_{rz}(r,z) = \mathcal{H}_1[S(\xi,z);\xi\to r], \tag{A17}$$
$$\sigma_{zz}(r,z) = \mathcal{H}_0[T(\xi,z);\xi\to r], \tag{A18}$$

where

$$\begin{bmatrix} 2GU \\ 2GV \\ -S \\ -T \end{bmatrix} = \begin{bmatrix} (\xi zA + C)\xi^{-1} \\ [(3-4\nu)A + \xi zA + C]\xi^{-1} \\ (1-2\nu)A + \xi zA + C \\ (2-2\nu)A + \xi zA + C \end{bmatrix} \exp(-\xi z). \tag{A19}$$

Appendix B. Solution to dual integral equations (25) and (26)

Taking $\alpha = -\frac{1}{2}$ and $\nu = 1$ in Eq. (4.2.21) in Sneddon (1966), the general solution to dual integral equations

$$\int_0^\infty \xi\bar{\psi}(\xi)J_1(\xi\rho)d\xi = F(\rho) \quad (0<\rho<1), \tag{B1}$$
$$\int_0^\infty \bar{\psi}(\xi)J_1(\xi\rho)d\xi = G(\rho) \quad (\rho>1), \tag{B2}$$

is given by

$$\bar{\psi}(\xi) = \frac{\sqrt{2\xi}}{\sqrt{\pi}}\int_0^1 \frac{1}{\sqrt{t}}J_{3/2}(\xi t)dt \int_0^t \frac{\tau^2}{\sqrt{t^2-\tau^2}}F(\tau)d\tau - \frac{\sqrt{2\xi}}{\sqrt{\pi}}\int_1^\infty t\sqrt{t}J_{3/2}(\xi t)dt\frac{d}{dt}\int_t^\infty \frac{1}{\sqrt{\tau^2-t^2}}G(\tau)d\tau. \tag{B3}$$

It should be pointed out that the original equation (4.2.21) in Sneddon (1966) contains a typo regarding the integral limits, which has been corrected in Eq. (B3).

Clearly, the dual integral equations (25) and (26) are a special case of (B1) and (B2) with

$$F(\tau) = c^2Q(\tau), \quad G(\tau) = -\frac{a^2\sigma_{th}\beta}{\tau}, \tag{B4}$$

where

$$Q(\tau) = \begin{cases} -\tau_f & (a/c<\tau\leqslant 1), \\ 0 & (0\leqslant\tau\leqslant a/c). \end{cases} \tag{B5}$$

Substituting Eqs. (B4) and (B5) into Eq. (B3) gives rise to

$$\begin{aligned}\bar{\psi}(\xi) &= -\frac{c^2\tau_f\sqrt{2\xi}}{\sqrt{\pi}}\int_{a/c}^1 \frac{1}{\sqrt{t}}J_{3/2}(\xi t)dt\int_{a/c}^t \frac{\tau^2}{\sqrt{t^2-\tau^2}}d\tau + \frac{a^2\sigma_{th}\beta\sqrt{2\xi}}{\sqrt{\pi}}\int_1^\infty t\sqrt{t}J_{3/2}(\xi t)dt\frac{d}{dt}\int_t^\infty \frac{1}{\tau\sqrt{\tau^2-t^2}}d\tau \\ &= -\frac{c^2\tau_f\sqrt{2\xi}}{\sqrt{\pi}}\int_{a/c}^1 \frac{1}{\sqrt{t}}J_{3/2}(\xi t)dt\int_{a/c}^t \frac{\tau^2}{\sqrt{t^2-\tau^2}}d\tau - \frac{a^2\sigma_{th}\beta\sqrt{2\pi\xi}}{2}\int_1^\infty \frac{1}{\sqrt{t}}J_{3/2}(\xi t)dt.\end{aligned} \tag{B6}$$

Since

$$J_{3/2}(x) = \sqrt{\frac{2}{\pi x}}\left(\frac{\sin x}{x} - \cos x\right)$$

and

$$\int_1^\infty \frac{1}{\sqrt{t}}J_{3/2}(\xi t)dt = \sqrt{\frac{2}{\pi}}\frac{\sin\xi}{\xi^{3/2}},$$

Eq. (B6) can be rewritten as

$$\bar{\psi}(\xi) = -\frac{2c^2\tau_f}{\pi}\int_{a/c}^1 \frac{1}{t}\left(\frac{\sin\xi t}{\xi t} - \cos\xi t\right)dt\int_{a/c}^t \frac{\tau^2}{\sqrt{t^2-\tau^2}}d\tau - \frac{a^2\sigma_{th}\beta\sin\xi}{\xi}. \tag{B7}$$

Appendix C. Solution to dual integral equations (50) and (51)

Taking $\alpha = \frac{1}{2}$ and $\nu = 1$ in Eq. (4.2.27) in Sneddon (1966), the general solutions to dual integral equations

$$\int_0^\infty \bar{\psi}(\xi) J_1(\xi\rho)d\xi = \mathrm{F}(\rho) \quad (0 \leqslant \rho \leqslant 1), \tag{C1}$$

$$\int_0^\infty \xi\bar{\psi}(\xi) J_1(\xi\rho)d\xi = G(\rho) \quad (\rho > 1), \tag{C2}$$

is given by

$$\bar{\psi}(\xi) = \frac{2}{\pi}\left\{\sin(\xi)\int_0^1 (1-t^2)^{-1/2}t^2F(t)dt + \int_0^1 (1-\tau^2)^{-1/2}\tau^2 d\tau \int_0^1 [\sin(\xi t) - \xi t\cos(\xi t)]F(t\tau)dt + \int_1^\infty t\sin(\xi t)dt \int_1^\infty (\tau^2-1)^{-1/2}G(t\tau)d\tau\right\}, \tag{C3}$$

where following relationships have been adopted:

$$J_{1/2}(x) = \sqrt{\frac{2}{\pi}}\frac{\sin x}{\sqrt{x}}, \quad J_{3/2}(x) = \sqrt{\frac{2}{\pi x}}\left(\frac{\sin x}{x} - \cos x\right).$$

Eqs. (50) and (51) are a specific case of dual integral equations (C1) and (C2) with

$$F(\rho) = c^2\sigma_{th}\beta\rho, G(\rho) = c^2Q(\rho), \tag{C4}$$

where

$$Q(\rho) = \begin{cases} \tau_f & (1 \leqslant \rho \leqslant a/c), \\ 0 & (a/c < \rho < \infty). \end{cases} \tag{C5}$$

Substituting Eqs. (C4) and (C5) into Eq. (C3) gives rise to

$$\begin{aligned}\bar{\psi}(\xi) = \frac{2}{\pi}\Bigg\{&\sin(\xi)c^2\sigma_{th}\beta\int_0^1 (1-t^2)^{-1/2}t^3dt + c^2\sigma_{th}\beta\int_0^1 (1-\tau^2)^{-1/2}\tau^3 d\tau\int_0^1 [\sin(\xi t) - \xi t\cos(\xi t)]t\,dt \\ &+\tau_f\int_1^{a/c} t\sin(\xi t)dt\int_1^{a/ct}(\tau^2-1)^{-1/2}d\tau\Bigg\} = \frac{2}{\pi}\left\{2c^2\sigma_{th}\beta\left[\frac{\sin\xi - \xi\cos\xi}{\xi^2}\right]\right. \\ &\left.+c^2\tau_f\int_1^{a/c} t\ln\left[\frac{a}{tc} + \sqrt{\frac{a^2}{t^2c^2}-1}\right]\sin(\xi t)dt\right\} = \frac{2}{\pi}c^2\tau_f\int_1^{a/c} t\ln\left[\frac{a}{tc} + \sqrt{\frac{a^2}{c^2t^2}-1}\right]\sin(\xi t)dt + \frac{4}{\pi}c^2\sigma_{th}\beta\left(\frac{\sin\xi}{\xi^2} - \frac{\cos\xi}{\xi}\right).\end{aligned} \tag{C6}$$

References

Arzt, E., Gorb, S., Spolenak, R., 2003. From micro to nano contacts in biological attachment devices. Proc. Natl. Acad. Sci. USA 100, 10603–10606.

Autumn, K., Liang, Y.A., Hsieh, S.T., Zesch, W., Chan, W.P., Kenny, T.W., Fearing, R., Full, R.J., 2000. Adhesive force of a single gecko foot-hair. Nature 405, 681–685.

Barthel, E., 1998. On the description of the adhesive contact of spheres with arbitrary interaction potentials. J. Coll. Interf. Sci. 200, 7–18.

Dugdale, D.S., 1960. Yielding of steel sheets containing slits. J. Appl. Mech. 8, 100–104.

Dundurs, J., 1969. Elastic interactions of dislocations with inhomogeneities. In: Mathematical Theory of Dislocations. American Society of Mechanical Engineering, New York, pp. 70–115.

Gao, H., Chen, S., 2005. Nanoscale flaw tolerance of a thin strip under tension. J. Appl. Mech. 72 (5), 732–737.

Gao, H., Yao, H., 2004. Shape insensitive optimal adhesion of nanoscale fibrillar structures. Proc. Natl. Acad. Sci. USA 101, 7851–7856.

Gao, H., Ji, B., Jäger, I.L., Arzt, E., Fratzl, P., 2003. Materials become insensitive to flaws at nanoscale: lessons from nature. Proc. Natl. Acad. Sci. USA 100, 5597–5600.

Gao, H., Ji, B., Buehler, M.J., Yao, H., 2004. Flaw tolerant bulk and surface nanostructures of biological systems. Mech. Chem. Biosys. 1, 37–52.

Gao, H., Wang, X., Yao, H., Gorb, S., Arzt, E., 2005. Mechanics of hierarchical adhesion structure of gecko. Mech. Mater. 37, 275–285.

Gladwell, G.M., 1980. Contact Problem in the Classical Theory of Elasticity. Sijthoff & Noordhoff, Netherlands.

Johnson, K.L., 1985. Contact Mechanics. Cambridge University Press, Cambridge, UK. 77 pp.

Persson, B.N.J., 2003. Nanoadhesion. Wear 254, 832–834.

Sneddon, I.N., 1966. Mixed Boundary Value Problems in Potential Theory. North-Holland, Amsterdam.

Tang, T., 2005. Can a fibrillar interface be stronger and tougher than a non-fibrillar one? J. R. Soc. Interf. 2, 505–516.